UNIVERSITÀ DEGLI STUDI DI NAPOLI FEDERICO II

SCUOLA DI MEDICINA E CHIRURGIA

Dipartimento di Scienze Biomediche Avanzate

Direttore Prof. Alberto Cuocolo

DOTTORATO DI RICERCA IN SCIENZE BIOMORFOLOGICHE E CHIRURGICHE

XXXIII CICLO

Coordinatore Prof. Alberto Cuocolo

TESI DI DOTTORATO

PROGNOSTIC ROLE OF CAF-1 COMPLEX IN UVEAL MELANOMA

RELATORE

Ch.ma Prof.ssa Stefania Staibano

CANDIDATO

Dott.ssa Rosa Maria Di Crescenzo

Introduction

Uveal Melanoma (UM) is a rare intraocular neoplasia. It arises from atypical melanocytes of the uveal tract, the concentric middle layer of the eye, consisting of the iris (in the anterior chamber of the eye), ciliary body, and choroid (in the posterior chamber). UM may originate in each of these layers, but the choroid is the most involved (85-90%). UM is the most common malignancy of the eye in adults and the most important type of non-cutaneous melanoma despite its rarity. UM and cutaneous melanoma share the same origin from melanocytes, but their etiology, pathogenesis, molecular profile, cytogenetic alterations, prognosis, and metastases development are entirely different[1]. In 1868 Hermann Kapp, a German ophthalmologist, described UM in his textbook "Die intraocularen Geschwulste' "[2]. Since this first description, UM has been deeply investigated, and

new information about the developmental molecular pathways of this neoplasia has been acquired constantly. Despite the growing body of research on its pathogenesis and the improvement of local treatment through radiotherapy and enucleation, UM is still a fatal disease, and patient survival is poor. Particularly about half of the patients develop metastases and, after metastasis development, the median survival is less than 12 months[3] and remained constant over the last four decades[4]. Therefore, scientific research focused on detecting new and effective prognostic factors in UM to identify high-risk patients early. In recent years, the knowledge of the relationship between specific genetic alterations and prognosis allowed the creation of hypothetic predictive evaluation systems to customize the patient's follow-up according to the metastatic risk. Unfortunately, the poor survival of UM patients and the ineffectiveness of tested treatments make the identification of reliable prognostic factors and new therapeutic protocols still urgent.

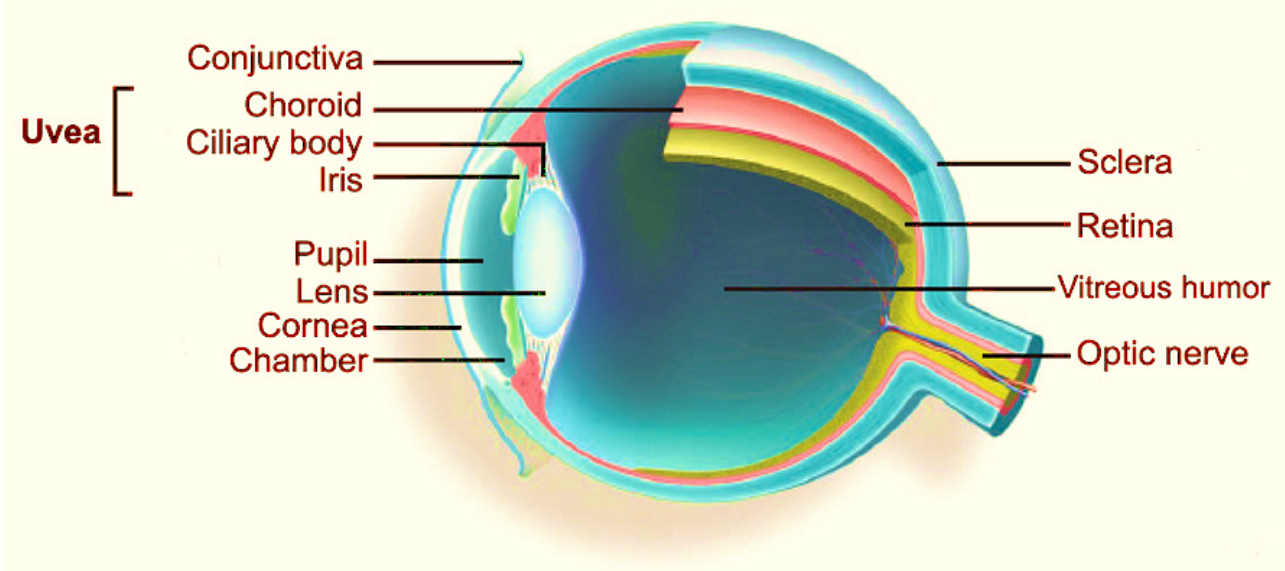

Figure 1: Eye anatomy.

Uveal Melanoma

Epidemiology

The eye is the most common site for melanoma after skin, and UM represents 3-5% of all melanomas. The incidence of UM in the United States is about 5.1 cases per million individuals[5]. Incidence varies between 2 and 8 per million person-years in Europe, depending on latitude, and is low in Africa and Asia, amounting to 0,2-0,3 cases per million person-years. At the diagnosis, the mean age is about 60-64 years[6], it is infrequent in people under 20 years old and extremely rare in children and newborns[7]. There is no sex predilection. As previously reported, 85-90% of UM

involves the choroidal layer, 5-8% originates from ciliary body melanocytes, and only 3-5% from the iris[8]. The disease is usually unilateral.

UM, prognosis partially depends on primary tumor location: iris melanoma is generally associated with a good prognosis, unlike choroidal and ciliary body melanoma.

Risk factors

UM may arise de novo or from melanocytes of uveal nevi and of congenital ocular/oculo-dermal melanocytosis. Oculodermal melanocytosis, also named Nevus of Ota, represents a significant risk factor of UM. Common risk factors are fair skin, light eyes, dysplastic nevus syndrome, and BAP1 tumor predisposition syndrome[9]. A recent study reported a significant association of UM with single nucleotide polymorphisms in the pigmentation genes HERC2, OCA2, and IRF4[10]. Despite World Health Organization classified UM as not associated with cumulative sun damage, many studies reported increased UM risk in patients with susceptibility to ultraviolet light and with cumulative ultraviolet light exposure. Moreover, the molecular characterization of UM suggests that the role of ultraviolet light in this neoplasia is marginal but not non-existent[11], especially in iris melanoma. Iris melanoma is more exposed to ultraviolet radiation because of its anterior position within the uveal tract and displays the genomic features associated with the ultraviolet radiation damage[12].

Another relevant risk factor is the presence of BAP1 (BRCA1 associated protein 1) mutations. BAP 1 is a tumor suppressor gene located on chromosome 3 (3p.21.1), and its germline mutations are associated with a novel cancer predisposition syndrome, called BAP-1 tumor predisposition syndrome. There is a high risk of developing uveal melanoma, malignant mesothelioma, renal cell carcinoma, cutaneous melanoma, and the BAP-1 inactivated melanocytic tumors in this syndrome.

The genetic origin of Uveal Melanoma

UM, unlike cutaneous melanoma, has a low mutational burden. The current knowledge of the molecular features of UM allowed to postulate a multistep carcinogenesis[13]. About 92% of UM present mutations in alpha G-protein subunits, GNAQ and GNA11, mutually.

The small fraction of UM, without GNAQ and GNA11 mutations, presents alterations of CYSLTR2 and PLCB4, activating the same G-protein-related pathway involved in regulating cell proliferation and survival. MAP kinase, protein kinase C and YAP pathways could be activated, and YAP, engaged in the Hippo pathway, promotes cell proliferation as an oncoprotein. These are early

events in UM oncogenesis, suggesting the relevant role of G protein signaling in UM development, but probably are not sufficient to lead malignant transformation[4].

The UM progression and the metastatic potential are associated with different genetic alterations, particularly loss of chromosome 3, mutations of the BAP1 gene, and amplification of the long arm of chromosome 8. Chromosome 3 monosomy is present in about 50-60% of UM and in more than 70% of metastasizing UM. Patients with chromosome 3-disomy have a 5-years survival rate of 90%[8]. 70% of UM with this chromosomal aberration develop metastasis and frequently present BAP1 gene mutations. BAP1 is located on chromosome 3 (3p.21) and encodes for a ubiquitin-carboxy-terminal hydrolase with deubiquitinase activity. It acts as an independent tumor suppressor gene that controls proteins involved in DNA damage repair, cellular differentiation, and proliferation[14]. BAP1 is a crucial regulator of cell cycle control and transcription because it acts with histone H2A. 30-40% of UM present somatic mutations of BAP1 and only 1-2% germline mutations[15]. BAP1 germline mutations could be associated with an early onset[16].

All tumors with BAP1 mutations have a genomic copy loss of chromosome 3, and BAP1 is a single copy gene presenting inactivating mutations.

BAP1 mutations are associated with a higher risk of developing secondary malignant tumors[17].

Gain of chromosome 6p and EIAF1AX and SF3B1 mutations may be present in patients with disomy 3 UM.

The eukaryotic translation initiation factor 1A, X-chromosomal (EIAF1AX), is a protein encoded by the EIF1AX gene, presenting missense mutations in 8-18,9% of primary UM. EIF1AX has a crucial role in the translation process. It is involved in the process of recognition and transfer of the start codon to the ribosomal subunit. How it is involved in UM development is still a matter of debate but has been demonstrated its association with a good prognosis[16].

In about 15% of UM cases, there are SF3B1 (Splicing factor 3B subunit 1) gene mutations. SF3B1 encodes for the splicing factor 3 subunit 1, a part of the spliceosome. The consequent splicing dysregulation modifies the transcriptional process with the production of aberrant transcripts. SF3B1 mutations are generally associated with earlier onset (54.4 years) and the risk of late metastasis development[18].

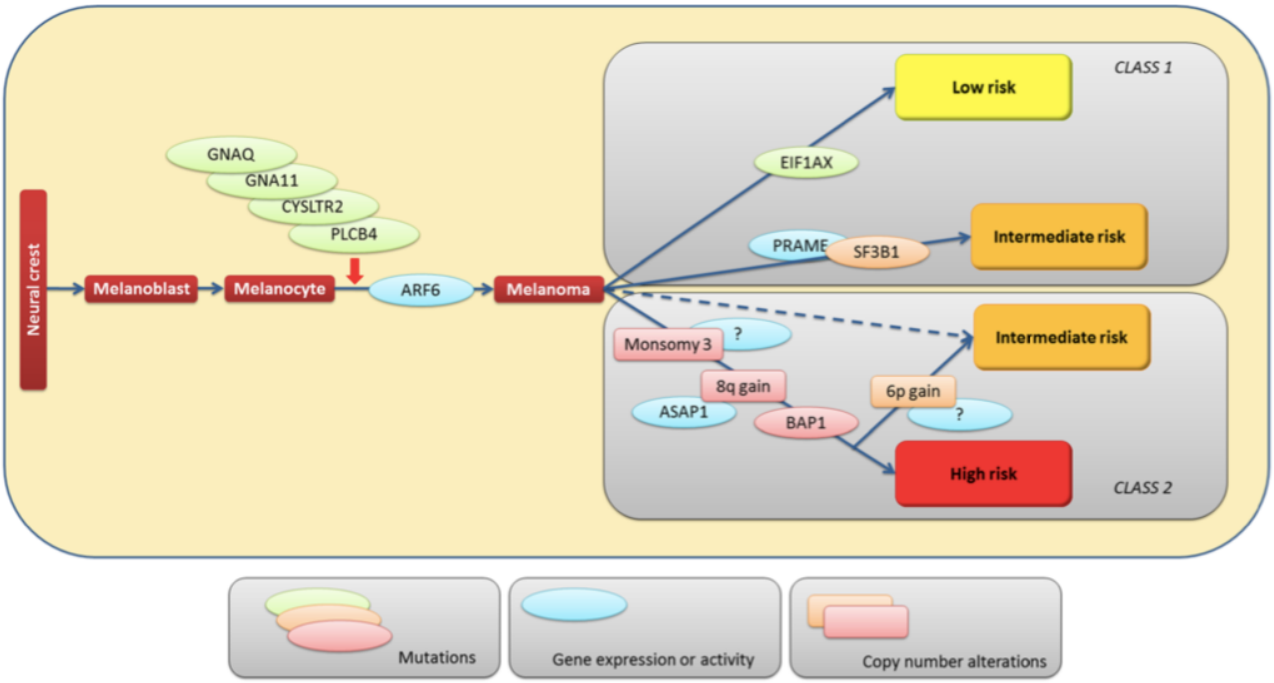

Figure 2: Multistep carcinogenesis of UM[13]

The genetic landscape of iris melanoma is not well explored, but some differences with posterior melanoma are already known. Iris melanoma rarely harbors BAP1 and SF3B1 mutations and occasionally presents BRAF mutations as cutaneous melanoma. It frequently shows loss of chromosome 3 and loss 9p and aberrations of chromosomes 1, 6, and 8[15].

Clinical presentation, diagnosis, and treatment

UM's clinical presentation depends on the tumor size and the ocular site involved, but it is frequently asymptomatic and diagnosed during a routine examination. Iris melanoma, typically visible through the cornea, often presents as a dark/white/pale brown lesion increasing in size and changing appearance[19]. Iris melanoma, characterized by multiple white nodules involving the entire iris surface, is called tapioca melanoma. It may infiltrate the ciliary body circumferentially, producing the so-called "ring melanoma" associated with a drainage blockage of the anterior chamber angle and elevation of the intraocular pressure[20] (secondary glaucoma). Iris melanoma may infiltrate the lens posteriorly, causing a sectorial cataract and deterioration of visual acuity. Posterior melanomas involve the choroid or the ciliary body, may appear as a dome-shaped, mushroom-shaped, or diffuse mass. Tumors are heavily pigmented in more than 50% of cases and present an overlying exudative retinal detachment, an important clinical sign. Posterior melanoma is associated with photopsia, floaters, and vision loss. Visual problems result when the

neoplasia affects the macula; instead, the involvement of the iridocorneal angle causes acute glaucoma with pain, loss of visual acuity, photopsia, and increased intraocular pressure[6].

In contrast, the disruption of ciliary epithelium (ciliary body melanoma) and the consequent reduction of aqueous humor induce eye hypotony. When the ciliary body is involved, the crystalline lens may be dislocated, causing astigmatism and unilateral cataract. Neural retinal detachment is present in approximately 75% of cases, and occasionally, may mask the underlying melanoma.

Proptosis is generally associated with extraocular extension. Rarely hyphema and vitreous hemorrhage occur as a consequence of tumor necrosis and disruption of blood vessels.

UM is generally detected through direct and indirect ophthalmoscopy. The tumor should be confirmed and measured using A-scan and B-scan ultrasonography. The OCT (optical coherence tomography) is helpful to investigate the effects of neoplasia on the overlying retina and evaluate the subretinal fluid[21].

Patients with uveal melanoma should complete the clinical staging with abdominal ultrasound, total-body CT, and complete blood tests, paying attention to the liver that is the first metastatic site.

Therapy of UM has changed over the past 30 years, and brachytherapy (plaque radiotherapy) and particle beam radiation are considered the first-line treatment for small and medium tumors. Surgery is reserved for large melanomas (diameter >20 mm, thickness >12 mm), tumors replacing >50% of the ocular globe, in cases of extensive extraocular extension, neovascular glaucoma, and

blind or painful eyes[22]. Orbital exenteration is limited to patients with extraocular extension and/or orbital invasion.

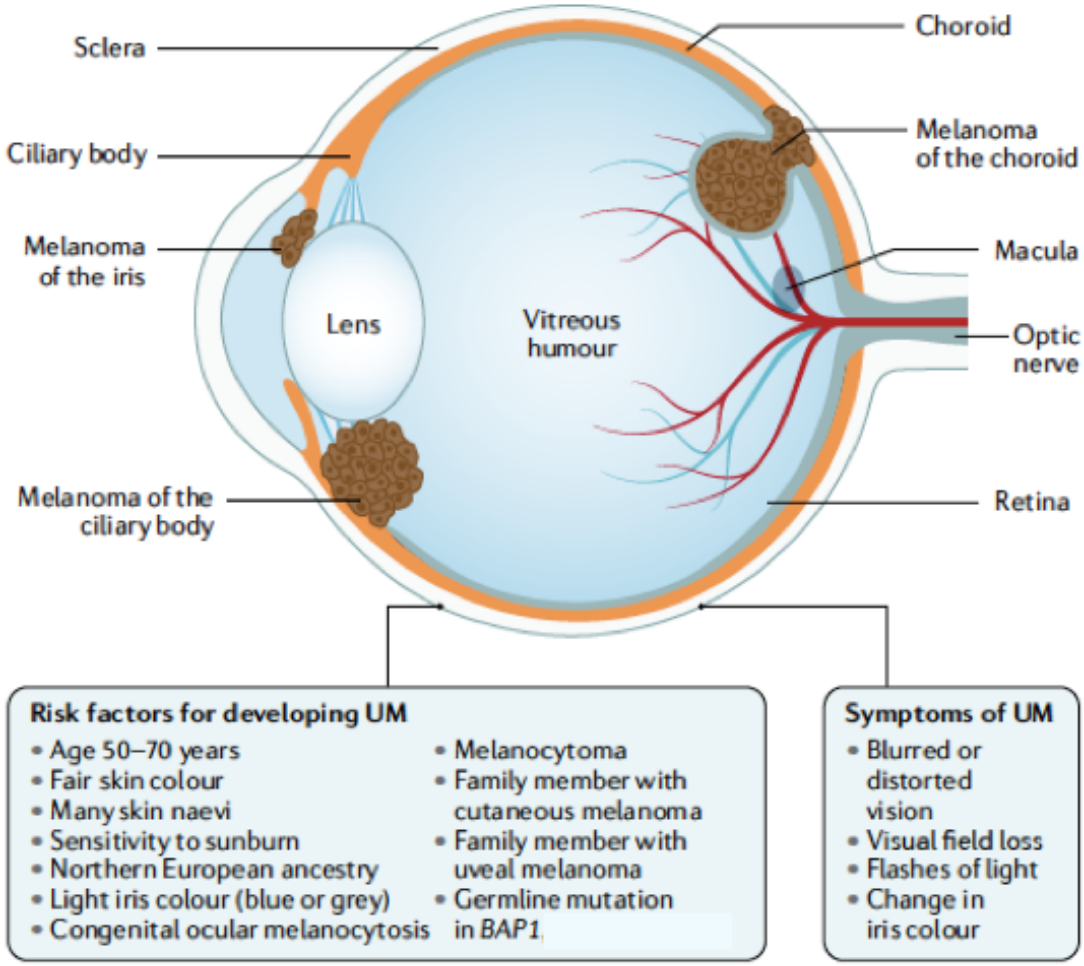

Figure 3: Development of UM, location, risk factors, and symptoms[23].

Histopathology of Uveal Melanoma

Microscopic description of uveal melanoma is traditionally based on the Callender modified system that identifies four types of tumors based on cytotype: type A spindle cell, type B spindle cell, epithelioid cell, and mixed cell. Spindle A cells are bland fusiform cells with central nuclei

containing central dark stripes/grooves.

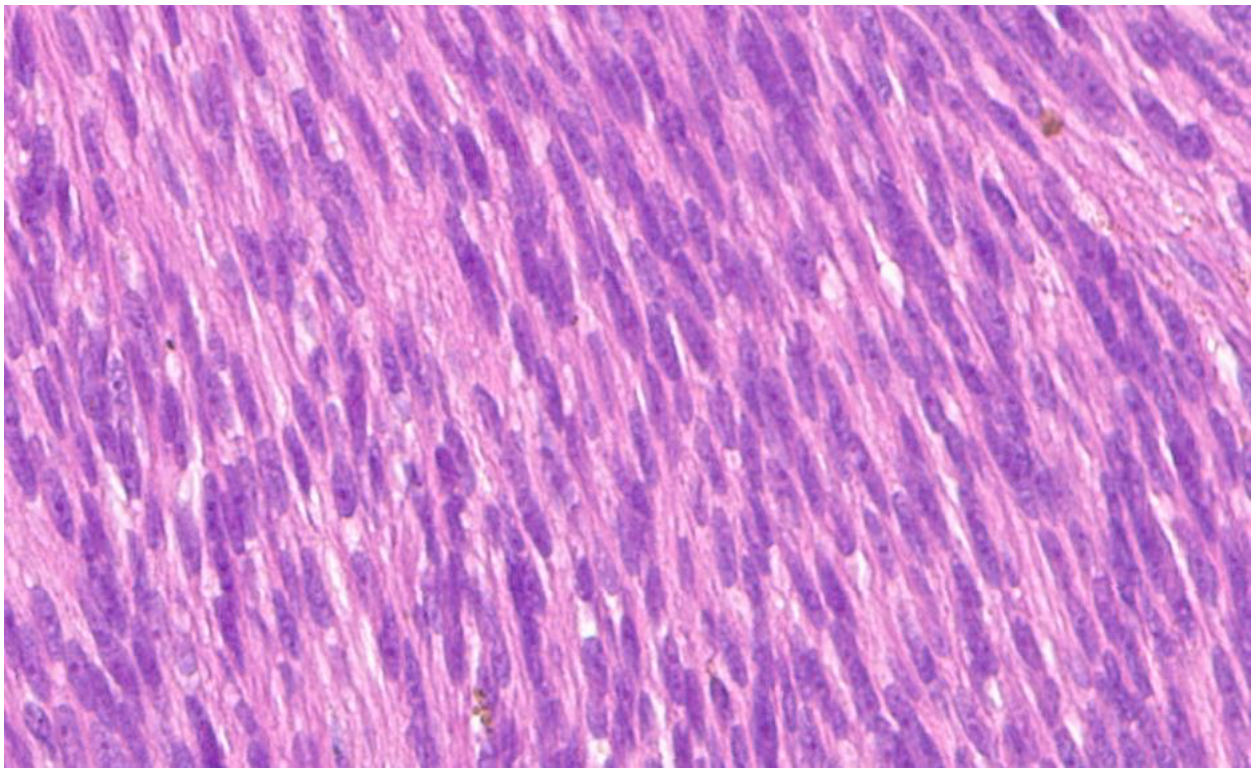

Figure 4: Histologic section showing spindle A cells sec.Callender.

Spindle B cells are fusiform and present central cigar-like nuclei with prominent nucleoli. The presence of spindle cells is associated with low metastatic risk and a good prognosis. Epithelioid cells are large, non-cohesive cells with abundant eosinophilic cytoplasm, central nuclei, and distinct nucleoli.

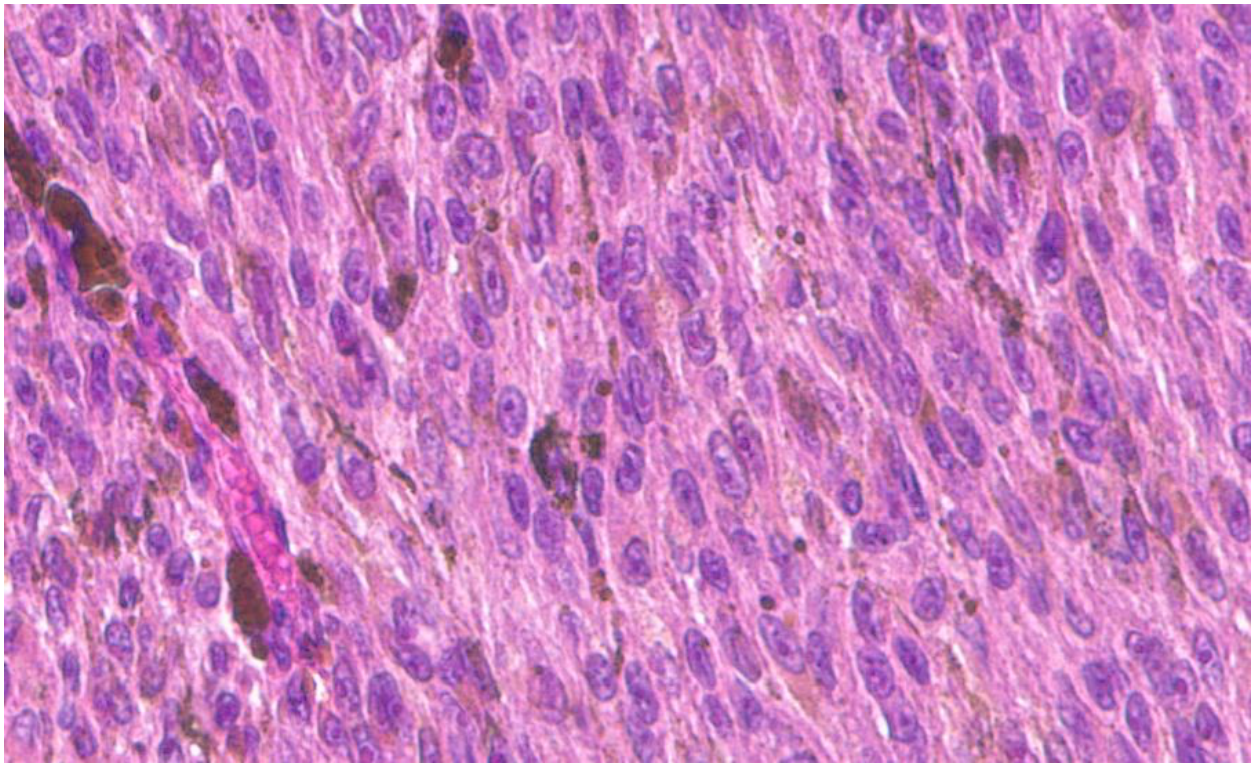

Figure 5: Histologic section showing spindle B cells sec. Callender.

Epithelioid cells are associated with a worse prognosis and a high metastatic risk.

Both components, spindle-B and epithelioid, characterize the mixed cell type, the most common type of melanoma. In the AJCC cancer staging manual 8th ed., the UM histological grading is based on assessing the prevalent cytotype. G1 is characterized by the presence of more than 90% of spindle cell melanoma. G2 are mixed cell melanomas constituted of more than 10% of epithelioid cells and less than 90% of spindle cells. G3 are epithelioid cell melanomas with a prevalence of epithelioid cells (more than 90%).

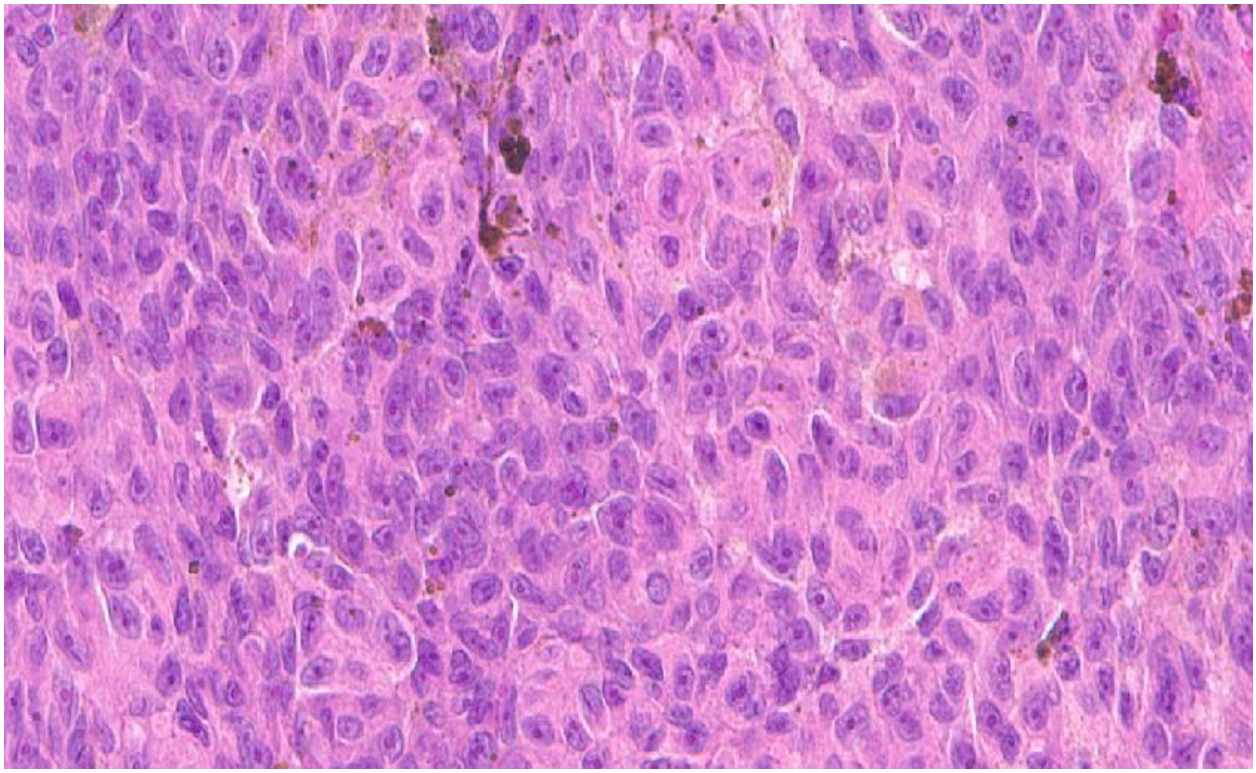

Figure 6: Histologic section of UM showing epithelioid cells.

The uncommon cytologic types of uveal melanoma are balloon cell, clear cell, signet ring cell, myxoid, small cell, oncocytic, and rhabdoid melanoma. Balloon cells are seen frequently in uveal melanoma previously treated with radiation therapy. UM may undergo spontaneous necrosis. UM is positive for HMB45 antigen, S100 protein, SOX-10, and Melan-A at the immunohistochemical examination, rarely required for the diagnosis. Ki-67, a nuclear proliferation marker, assesses the proliferative activity and has a prognostic significance.

UM staging, AJCC 7th edition

The AJCC cancer staging manual provides a precise classification for numerous solid cancers and is also called TNM classification. For UM, the staging system consists of three parameters: tumor (T), node (N), and metastasis (M). The T categories assessment for iris melanoma staging is founded on the tumor extension, measured in clock hours of involvement, basal dimensions, tumor thickness, and the presence of glaucoma.

4.1 Definition of Primary Tumor (T)

✓	*T Category*	*T Criteria*
	TX	Primary tumor cannot be assessed
	T0	No evidence of primary tumor
	T1	Tumor limited to the iris
	T1a	Tumor limited to the iris, not more than 3 clock hours in size
	T1b	Tumor limited to the iris, more than 3 clock hours in size
	T1c	Tumor limited to the iris with secondary glaucoma
	T2	Tumor confluent with or extending into the ciliary body, choroid, or both
	T2a	Tumor confluent with or extending into the ciliary body, without secondary glaucoma
	T2b	Tumor confluent with or extending into the ciliary body and choroid, without secondary glaucoma
	T2c	Tumor confluent with or extending into the ciliary body, choroid, or both, with secondary glaucoma
	T3	Tumor confluent with or extending into the ciliary body, choroid, or both, with scleral extension
	T4	Tumor with extrascleral extension
	T4a	Tumor with extrascleral extension ≤5 mm in largest diameter
	T4b	Tumor with extrascleral extension >5 mm in largest diameter
Note: Iris melanomas originate from, and are predominantly located in, this region of the uvea. If less than half the tumor volume is located within the iris, the tumor may have originated in the ciliary body, and consideration should be given to classifying it accordingly.		

Figure 7: Staging of Iris Melanoma[24]

For choroidal and ciliary body melanoma, the size category classification is essential for the T parameter. The size category is a classification scheme combining the largest basal diameter and thickness of the tumor.

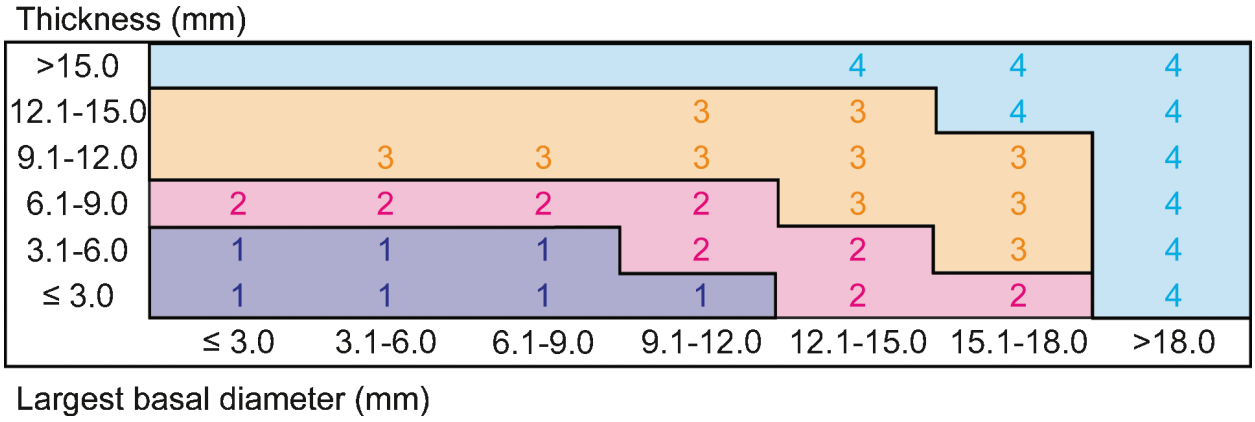

Figure 8: Size classification for ciliary body and choroidal melanoma, based on thickness and largest basal diameter[24]

Beyond the anatomic extent of choroidal and ciliary body melanomas, expressed as tumor size, T categories describe the involvement of the ciliary body and the extra-scleral extension. Consequently, within each T category, subcategories correspond to the presence of ciliary body involvement and/ or extra-scleral extension ≤5 mm, or extra-scleral extension > 5mm.

The node staging is based on one or more lymph node metastasis or tumor deposits in the orbit without contiguity with the eye. The M parameter depends on the metastatic nodule size[24].

Several studies have explored the predictive capability for UM of AJCC classification and demonstrated the significant association of T categories with poor survival outcomes[25].

✓	T Category	T Criteria
	TX	Primary tumor cannot be assessed
	T0	No evidence of primary tumor
	T1	Tumor size category 1
	T1a	Tumor size category 1 without ciliary body involvement and extraocular extension
	T1b	Tumor size category 1 with ciliary body involvement
	T1c	Tumor size category 1 without ciliary body involvement but with extraocular extension ≤5 mm in largest diameter
	T1d	Tumor size category 1 with ciliary body involvement and extraocular extension ≤5 mm in largest diameter
	T2	Tumor size category 2
	T2a	Tumor size category 2 without ciliary body involvement and extraocular extension
	T2b	Tumor size category 2 with ciliary body involvement
	T2c	Tumor size category 2 without ciliary body involvement but with extraocular extension ≤5 mm in largest diameter
	T2d	Tumor size category 2 with ciliary body involvement and extraocular extension ≤5 mm in largest diameter
	T3	Tumor size category 3
	T3a	Tumor size category 3 without ciliary body involvement and extraocular extension
	T3b	Tumor size category 3 with ciliary body involvement
	T3c	Tumor size category 3 without ciliary body involvement but with extraocular extension ≤5 mm in largest diameter
	T3d	Tumor size category 3 with ciliary body involvement and extraocular extension ≤5 mm in largest diameter
	T4	Tumor size category 4
	T4a	Tumor size category 4 without ciliary body involvement and extraocular extension
	T4b	Tumor size category 4 with ciliary body involvement
	T4c	Tumor size category 4 without ciliary body involvement but with extraocular extension ≤5 mm in largest diameter
	T4d	Tumor size category 4 with ciliary body involvement and extraocular extension ≤5 mm in largest diameter
	T4e	Any tumor size category with extraocular extension >5 mm in largest diameter

Notes:

1. Primary ciliary body and choroidal melanomas are classified according to the four tumor size categories defined in Figure 67.1
2. In clinical practice, the largest tumor basal diameter may be estimated in optic disc diameters (DD; average: 1 DD = 1.5 mm), and tumor thickness may be estimated in diopters (average: 2.5 diopters = 1 mm). Ultrasonography and fundus photography are used to provide more accurate measurements.
3. When histopathologic measurements are recorded after fixation, tumor diameter and thickness may be underestimated because of tissue shrinkage.

Figure 9: Staging of choroidal and ciliary body melanoma[24]

Prognostic factors in UM

Despite progress in diagnosis and treatment of primary disease, UM overall survival rates remained stable over the last years. Only 3% of patients have metastases at the time of the diagnosis, but up to 50% of patients develop metastases during follow-up. The mortality rate is about 31% at five years, increasing to 52% at 35 years[16].

In recent years, several clinical, histological, and molecular factors acquired prognostic relevance in UM. Estimation of metastatic risk could help in planning patient-tailored systemic surveillance for early detection of metastasis.

The intraocular location of UM with ciliary body involvement is independently associated with metastatic risk. Conversely, tumors confined to the iris have the most favorable prognosis[24].

The AJCC staging considers the tumor size, the ciliary body invasion, and the extraocular extension and has a relevant prognostic role. Mainly T category is strongly predictive of metastatic disease. The ten-year metastatic rate in T1 tumors is 15%, increasing to 25% for T2 and 49% for T3. UM with the T4 stage has a 63% metastatic rate[26,27].

Moreover, cell type is an independent prognostic factor. Epithelioid cells are associated with the shortest survival times and a higher metastatic risk.

A high number of mitotic figures counted per 40 high-power fields (HPF 40x), close microvascular loops, high microvascular density, and the presence of tumor-infiltrating lymphocytes and macrophages are all associated with higher metastatic risk and considered relevant prognostic factors[24].

Although clinical and histopathological parameters are effective predictors in UM, the mutational landscape has become relevant in metastatic risk prediction.

Chromosome 3 monosomy is a relevant cytogenetic alteration in metastatic UM. It is related to negative histopathological prognostic factors and poor prognosis. UM could harbor partial chromosome 3-monosomy having a better prognosis compared to the complete one. Generally, it is associated with inactivating mutations of BAP1, located on chromosome 3.

In UM, BAP1 mutations are present in 84% of metastasized tumors. BAP1 depletion increases the amount of transmigration in uveal melanoma cells promoting the metastasizing process[28]. Therefore, loss of BAP1 is a crucial event to metastasis development in UM.

A decrease in disease-free survival is described in tumors with the combination of BAP1 mutations and the 3-monosomy[29] particularly. Besides BAP1, alterations of SF3B1 and EIF1AX are related to prognosis and are present in a mutually exclusive manner. 22% of UM with SF3B1 mutations present monosomy of chromosome 3. Tumors with SF3B1 mutations have an intermediate risk of late-onset metastasis due to their effects on splicing[19]. EIF1AX mutations are never found in tumors with chromosome 3 monosomy and are associated with a good prognosis. The second most common chromosomal aberration after chromosome 3 monosomy is the 8q amplification equally associated with poor prognosis. 8q copy number variations are present in 79% of UM cases.

Gain of chromosome 6 and 1p loss are other chromosomal aberrations reported in UM.

1p loss generally occurs in association with 3-monosomy and is related to reduced survival.

Gain of chromosome 6 is considered a protective cytogenetic alteration in UM associated with good prognosis and non-metastatic disease[16].

The growing body of knowledge about the correlation between cytogenetic alterations and prognosis in UM leads to the development of several classifications and prognostication methods. Recently a large comprehensive TGCA study with an extensive comparison of the available prognostic parameters and clinical outcomes proposes a new molecular classification based on four molecularly distinct, clinically relevant subtypes. Two subclasses are characterized by 3-

disomy (D3) and good prognosis; the other two classes are associated with 3-monosomy (M3) and a worse prognosis.

These classes previously identified with Arabic numbers (1,2,3,4) were relabeled with the alphabetic letters A, B, C, and D. Class A includes tumors with 3-disomy, class B 3-disomy and 8q gain, class C 3-monosomy, and 8q gain, and class D 3-monosomy and 8q gain (multiple)[30,31].

TCGA classification is a simple, accurate, and robust predictor of UM metastasis and will allow a better understanding of UM behavior[25] and is the evolution of all prognostics parameters, including the GEP (gene expression profiling). GEP is a predictive test based on 15 genes (12 discriminating genes and three controls) expression profiling based on mRNA analysis. It divides UM into two prognostically significant groups without regard to chromosomal status. Class 1 tumors are linked to a better prognosis presenting a gene expression profiling resembling normal uveal melanocytes. Class 2 tumors present a transcriptome of primitive neural/ectodermal stem cells and poor prognosis[32]. Compared with other prognostic parameters, including chromosome 3 analysis, GEP resulted as the most relevant predictive test except for the gene expression of PRAME (preferentially expressed antigen in melanoma). PRAME encodes for a "tumor-associated antigen" that influences cell differentiation and apoptosis and is considered an independent prognostic biomarker that identifies increase metastatic risk in class 1 patients.

PRAME is never associated with 3-monosomy but frequently related to SF3B1 mutations[33].

Prediction in UM achieved high precision, but these prognostication systems are tested and validated on FNAB (Fine Needle Aspiration Biopsy). Tumor biopsies in UM present some limitations, especially regarding sample representativity. The spatial and temporal tumor heterogeneity is a well-demonstrated feature of medium/large UM, which may interfere with tailored prognostication and ad prediction of tumor behavior performed of FNAB[34].

Therapy of metastatic UM

Despite the predictive systems, surveillance is the essential tool to detect metastasis early in patients with UM. Therefore, a rigorous and extended (10 years at least) follow-up including serum tests and imaging techniques (MRI with contrast and the US) is strongly recommended. The most common metastatic site is the liver, followed by lung, bone, skin/soft tissue, and lymph nodes, in order of decreasing prevalence[22]. Surgical resection of liver metastases in selected patients is considered the most effective approach, with median overall survival more significant

than 20 months[22]. Unfortunately, patients with resectable metastases are less than 10%, and liver metastases are frequently multiple involving both liver's lobes[16]. Alternative liver approaches aiming to reduce side effects of systemic treatment are Transarterial Chemoembolization, Selective Internal Radiation Therapy, Isolated Hepatic Infusion (IHP), Percutaneous Hepatic Perfusion (PHP), and Hepatic Artery Infusion (HIA). These therapeutic strategies are not associated with a relevant survival improvement. For UM, different systemic therapies have been tested in clinical trials. UM is resistant to systemic cytotoxic chemotherapy (dacarbazine, temozolomide, cisplatin, bendamustine, treosulfan, fotemustine-based regimens, and others) with a response rate ranging from 0% to 15%[35]. UM does not harbor mutations of BRAF or NRAS but presents oncogenic mutations of GNAQ and GNA11, activating the MAPK pathway. Inhibitors of this pathway like MEK inhibitor (selumetinib and trametinib) showed clinical benefit in a small proportion of patients. Checkpoint immunotherapy options for uveal melanoma include anti-PD1 and Anti-CTLA4 agents. Ipilimumab and tremelimumab are anti-CTLA4 agents that resulted similarly to conventional systemic chemotherapy in patients with uveal melanoma. Despite the variable response rate, anti-PD1 systemic therapy (monotherapy or combination) with ipilimumab and nivolumab is recommended in patients with metastatic UM. Since there aren't any effective treatments, improving the overall survival in metastatic UM, participation in clinical trials is currently the preferred option and is strongly recommended[22].

Chromatin Assembly Complex (CAF-1)

Introduction

In eukaryotic cells, DNA replication is a complicated process comprising two phases: copy of DNA and formation of accurate chromatin structures. Chromatin is a complex of DNA and proteins, called histones, with the essential function of packing DNA in compact and dense structures. The chromatin organization prevents DNA damage and regulates DNA replication and gene expression. The fundamental element of chromatin is the nucleosome consisting of a DNA segment wrapped around a histone octamer composed of two copies of each histone protein (H2A, H2B, H3, and H4). Nucleosome probably preserves epigenetically inherited information, and the chromatin complexity is essential to protect DNA integrity. Nucleosome assembly is critical for genomic stability, and it follows the DNA synthesis with the help of some proteins such as NAP-1 and the CAF-1 complex.

Structure and function of the CAF-1 complex

CAF-1 is a heterotrimeric complex with the peculiar function assemble H3 and H4 histones onto the newly synthesized DNA. It consists of three subunits named CAF-1 p150, CAF-1 p60, and CAF-1p48. The name of every single subunit depends on the molecular weight following gel electrophoresis[36].

Since the first studies conducted in vitro, CAF-1 demonstrated its central role in synthesizing the nucleosome during the DNA synthesis phase (S). Particularly the CAF-1 complex leads the translocation of the histones, H3 and H4, into the nucleus and facilitates their deacetylation and integration onto the newly synthesized DNA. The first step of this process consists of the interaction of CAF-1 p60 with histones H3 and H4 complexed with ASF1, a chaperonin that maintains direct contact with histone proteins.

The p60 / ASF1 / H3 / H4 complex binds the p150 subunit. This subunit targets the CAF-1 complex that interacts with the replication fork through PCNA (proliferating nuclear cell antigen). PCNA forms a sliding clamp on the replicating DNA and is the scaffold for different factors such as DNA polymerase. These interactions allow the CAF1 complex to assemble the histones H3/H4 to the DNA in the replication fork. The p48 subunit interacts with histone H4 through two α-helical domains independently from CAF-1 and cooperates with the Retinoblastoma protein (Rb)[37].

CAF1p60 deletion in replicating cells induces cell death in 24 hours due to the failure of the replication process and the accumulation of DNA damage[38].

Moreover, the CAF-1 complex is involved in DNA repair. In particular, p150 subunit has a role during the nucleotide excision repair (NER) with PCNA[39]. Moreover, it also has a PCNA-independent function in the double-strand break (DSB) repair[40].

CAF-1 complex has a function in nucleosome assembly and heterochromatin maintenance and a significant role in proliferative tissues.

Several studies showed that CAF-1p60 has a prognostic role in different malignancies. Particularly, CAF-1p60 overexpression is associated with poor prognosis, aggressive behavior, and metastasis development in the prostate, laryngeal, breast, and oral carcinomas, as well as in cutaneous melanoma[41,42].

CAF-1 p60 presented low expression levels in normal melanocytes, mid-levels in radial growth phase melanoma, and high levels in vertical growth phase melanoma, suggesting a correlation with melanoma aggressiveness[43].

Moreover, a recent study individuates the association between p150 subunit expression and poor prognosis in cervical cancer, revealing its potential prognostic role associated with its crucial role in cell proliferation[44].

A recent study of the expression of some genes involved in DNA replication and repair highlighted the overexpression of the PCNA gene in a significant proportion of UM with poor prognosis. This increase is not associated with specific gene mutations, suggesting a cellular mechanism to bypass the replication stress causing the replication fork collapse. Therefore, also CAF1 complex is probably involved in this process[45].

Aim of the study

The CAF-1 complex promotes the nucleosome assembly on the newly synthesized DNA, regulating the chromatin assembly and stabilization, and is involved in the DNA replication process[37].

It has been demonstrated that CAF-1 may be helpful to predict the clinical outcome in patients with malignant tumors, particularly in cutaneous melanoma.

This research investigates the potential prognostic role of p60 and p150 subunits of CAF-1 in UM, considering the critical role of CAF-1 subunits as a relevant predictive marker for cutaneous melanoma. Moreover, we compared the immunohistochemical expression of CAF-1 subunits with the expression of BAP1 in selected UM cases. Nuclear BAP1 stain is considered a significant independent predictor of metastatic disease in UM.

Materials and Methods

Case Series and Study Population

Formalin-fixed, paraffin-embedded tissue blocks of 133 UM were collected. All patients included in this study underwent enucleation between 1990 and 2018. We retrieved the specimens from the archives of the Pathology Section of the Department of Advanced Biomedical Sciences, University of Naples "Federico II," and of the Department G.F. Ingrassia, Section of Anatomic Pathology, University of Catania. TMAs were cored all together at the same time. We excluded 5/133 cores due to core loss during processing. We ran the visual analysis on 128 cores. The clinical data and

pathological features of the tumors are reported in table 1. Updated follow-ups were available for 121 cases. All tumor samples were staged according to the 8th AJCC staging manual[24].

The study population was mainly composed of men (50,3%) with a mean age of 63,15 years. A consistent proportion of the selected cases were choroidal melanomas (81%), and 6 cases presented extraocular extension. 23 patients had previously been treated with brachytherapy and underwent enucleation for recurrence.

Table 1: Descriptive table of the study population.

Gender (M)	67 (50,3%)
Age (years)	63±13
Location	
Choroid	109 (81%)
Choroid and Ciliary Body	16 (12%)
Iris and ciliary body	1 (0,7%)
Ciliary Body	1 (0,7%)
Extraocular Extension	6 (4,5%)
LBD (cm)	1,38 ±0,55
Thickness (cm)	0,82±0,4
Cellularity	
mixed	76 (57%)
epithelioid	36 (27%)
spindle	21 (15%)
TNM (T1/2/3/4)	
T1	23(17%)
T2	35(24%)
T3	47(33%)
T4	28(19%)
Brachytherapy pre-enucleation	23 (17,2%)

TMAs construction

Two expert pathologists reviewed hematoxylin-Eosin (H-E) sections of all UM cases and selected the most representative areas for each one. The selection was conducted excluding hemorrhagic, necrotic, and, if possible, hyperpigmentation areas and considering intra-tumor heterogeneity[46]. Three-mm cores, derived from the most representative areas of each tumor (from 2 to 3 cores per tumor depending on tumor size), were taken by a manual tissue-array instrument (Tissue-Tek Quick-Ray, Sakura Finetek, Torrance, CA, United States). The tissue cores were put into empty "recipient" paraffin blocks with 30 holes each. Subsequently, the recipient blocks were placed on metal base molds. The paraffin-embedding was performed as follows: the blocks were heated at

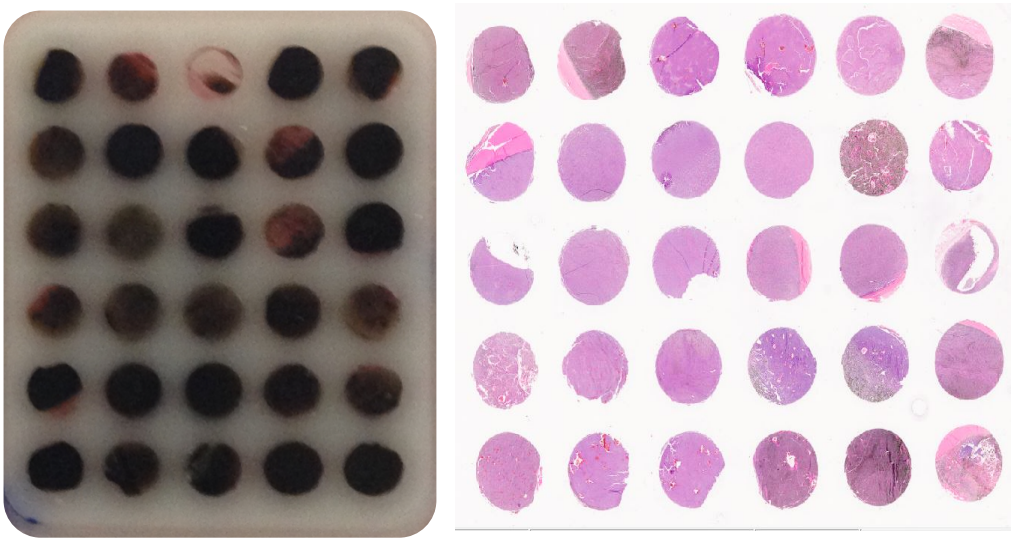

Figure 10: A TMA and its corresponding H&E section.

42°C for 10 min, and their surface was flattened by pressing a clean glass slide on them. We obtained nine TMAs (tissue Microarray). Two 4-µm sections were cut from each with a standard microtome. The first section was stained with H&E to confirm the correct execution of the procedure (presence and integrity of tumor cores).

Immunohistochemistry

A 4-µm tissue section from each TMA was transferred onto TOMO® IHC Adhesive Glass Slides (Matsunami Glass Ind., Ltd., Japan). Deparaffinized TMA sections were treated with sodium citrate or EDTA buffers (pH 6.0 and pH 7.8, respectively) for antigen retrieval. To prevent the non-specific bindings, sections were incubated with Dual Endogenous Enzyme Block (Dako Diagnostics, Glostrup, Denmark) at room temperature and with Protein-block, Serum-Free (Dako Diagnostics, Glostrup, Denmark) followed by a rinse with a suitable wash buffer. Consequently, sections were incubated overnight at 4°C with the anti-CAF-1/p60 antibody (SS53 - ab8133, Abcam, Cambridge,

MA, USA, dilution 1:100) and CAF1 p150 (EPR5576, Abcam, Cambridge, MA, USA, dilution 1:100) for one hour. After the standard streptavidin-biotin-peroxidase complex application (labeled streptavidin-biotin-complex/ horse-radish AP; DAKO, Carpenteria, CA) was used Ultra View Universal Alkaline Phosphatase Red Detection Kit (Ventana Medical Systems, Inc., Tucson, AZ, United States) as an indirect detection system. This technique produces a red precipitate that is readily detected by light microscopy.

Hematoxylin was used for nuclear counterstaining; sections were then mounted and cover-slipped with a synthetic mounting medium (Entellan, Merck, Germany).

BAP1 immunohistochemistry was performed on paraffin tissue sections with the fully automated Ventana Benchmark Ultra platform (Ventana Medical Systems Inc., Tucson, AZ, United States) using a red chromogen according to the manufacturer protocol. After the standard procedures of deparaffinization and sections antigen retrieval, the sections were incubated for one hour with BAP1 antibody (1:50 dilution; Santa Cruz Biotechnology, USA). This process was followed by incubation with hematoxylin counterstain.

Immunohistochemical evaluation

Determination of CAF1-p60 and CAF-1 p150 nuclear expression was assessed following a new approach, more accurate than the semiquantitative method used until now.

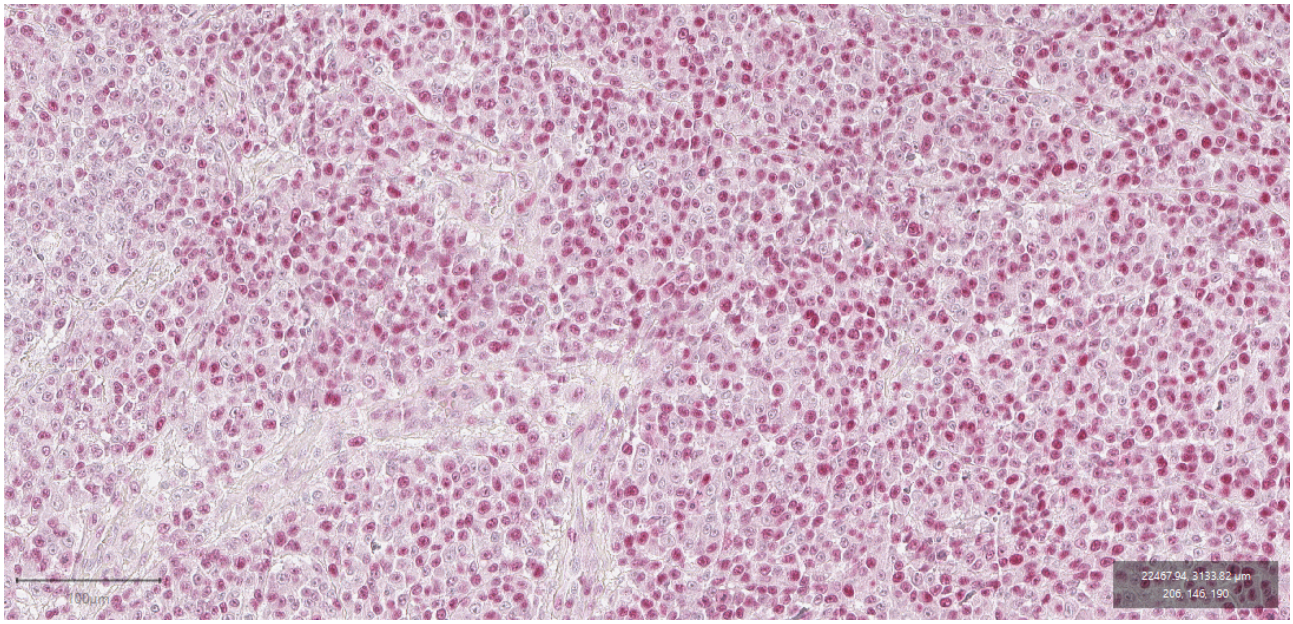

Figure 11: Epression of CAF-1p150 in about 48% of tumor cells with strong intensity.

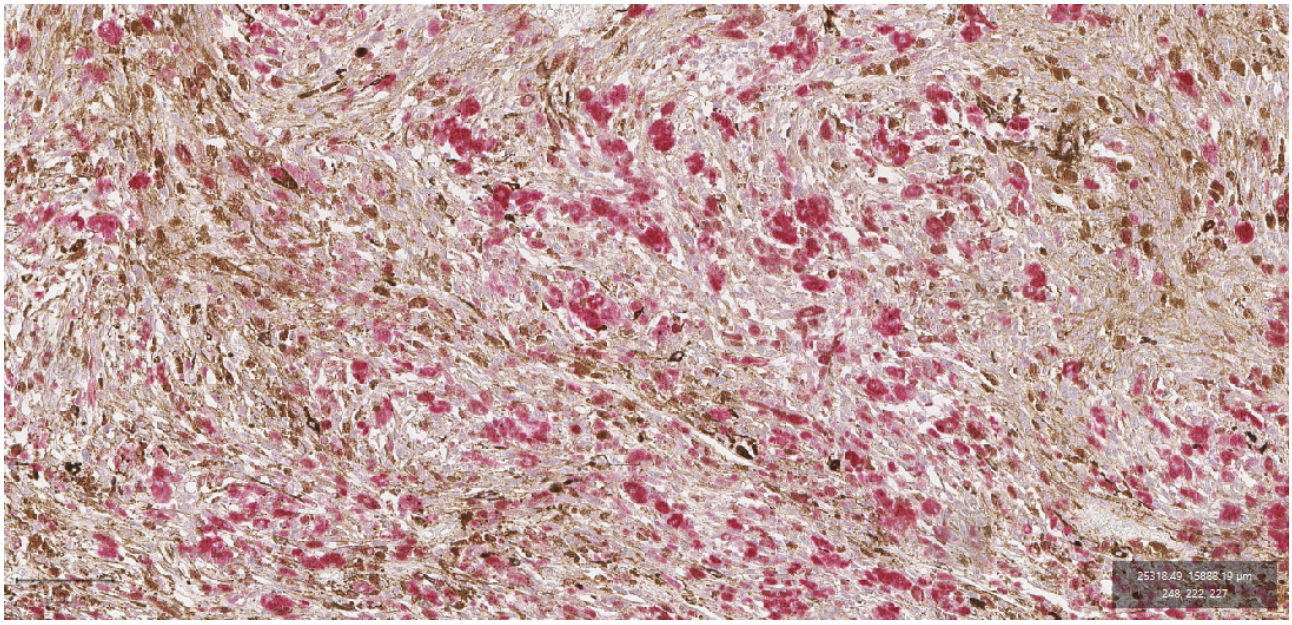

Figure 12: Negative immunohistochemical expression of CAF-1 p150.

This new scoring system is based on two parameters: the percentage of positive nuclei and the staining intensity.

The percentage of positive cells was evaluated in 5 high-power fields, counting 100 cells.

The staining signal was recorded as weak, intermediate, or strong.

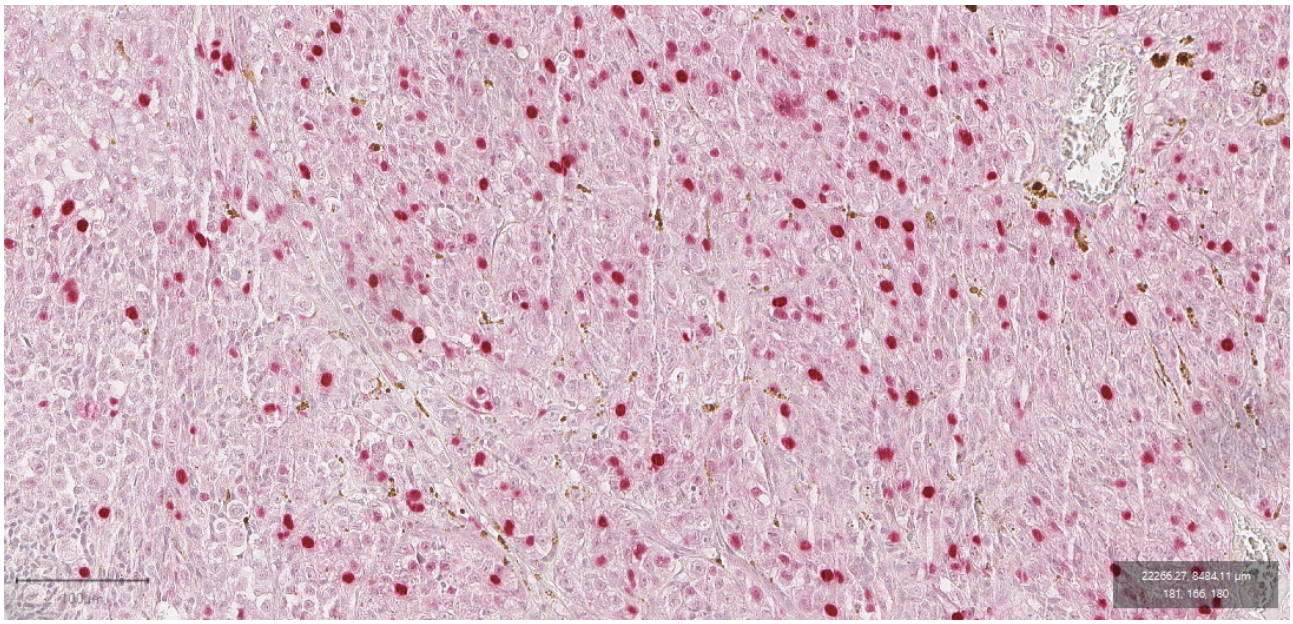

Figure 13: Immunohistochemical expression of CAF-1 p60 in about 21% of neoplastic cell with strong intensity.

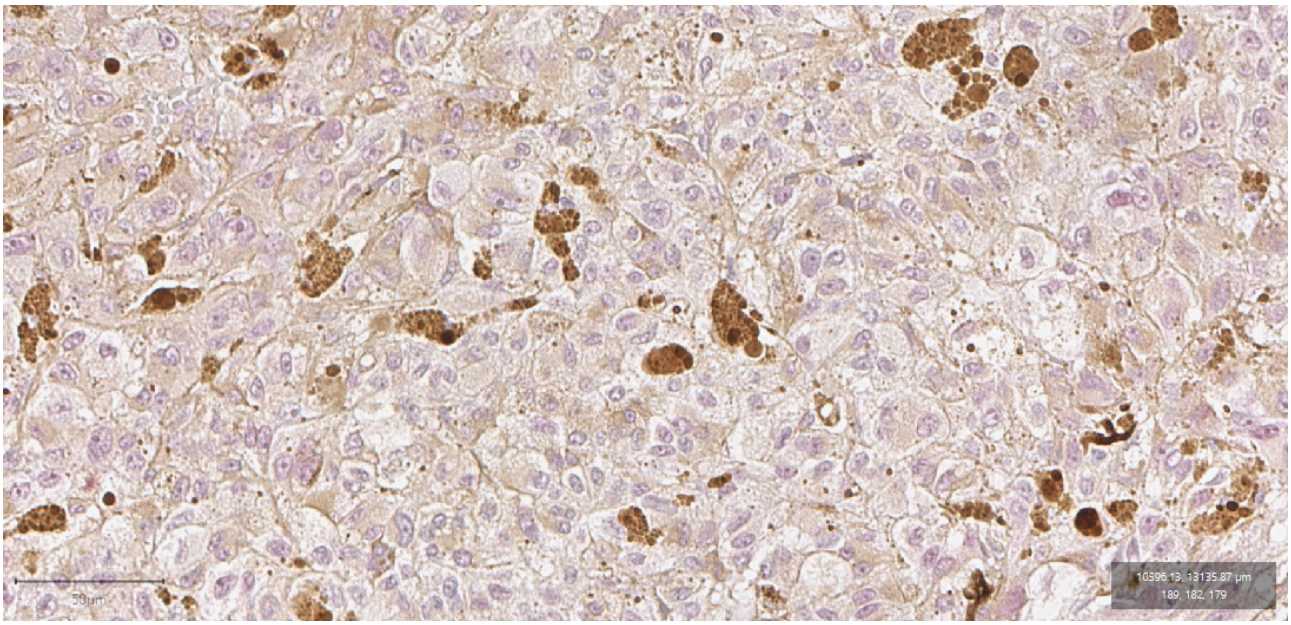

Figure 15: Negative immunostaining for CAF-1 p60.

The nuclear immunoreactivity of BAP1 was evaluated by counting the positive cells on 100 cells in 3 high-power fields. According to the literature, Cases were classified in Bap1 low and BAP1high, considering 33% of positive tumor nuclei as a cut-off[47].

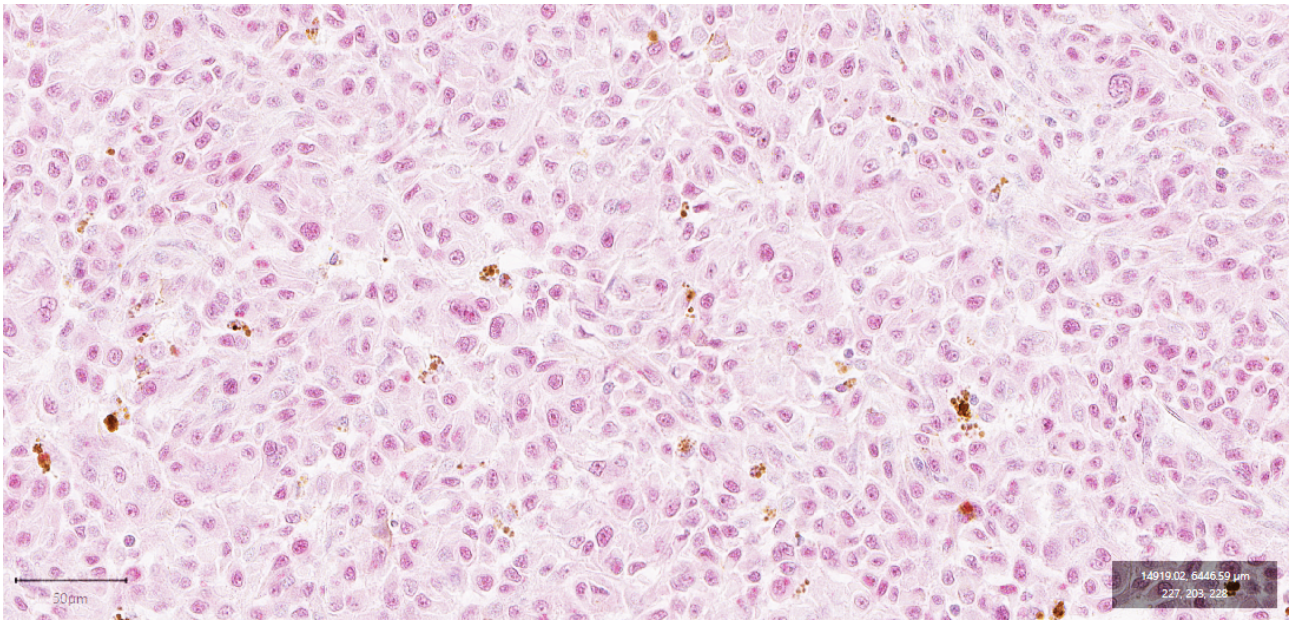

Figure 14: BAP1 nuclear expression.

Statistical Analysis

SPSS software (IBM Corp. Released 2013. IBM SPSS Statistics for Windows, Version 25.0. Armonk, NY, United States) was used for statistical analysis. Continuous variables are expressed as means +/- standard deviation. Multiple-group comparisons were performed using the analysis of variance

and Tukey post-hoc test. Frequencies were compared using the chi-square test. Optimal CAF-1 p60 and CAF-1 p150 cut-off values for predicting disease-free survival were assessed through receiver-operating curve (ROC) analysis and Youden's index. Survival analysis was performed testing the differences between Kaplan–Meier survival curves with the log-rank test.

Cases with unavailable follow-up data were excluded from the statistical analysis.

Results

Of 128 evaluable UM cases immunostained for CAF-1p150, 40 were negative and 88 positives with variable intensity and a mean percentage of positive cells of 9,4% ± 0,10. CAF-1 p60 immunostaining was negative in 27 cases and positive in 101 cases with varying intensity and a mean rate of positive cells of 7,86% ± 0,06.

BAP-1 was positive in 26 cases (7 <33% and 19 >33%) and negative in 86 cases. 16 cases were not evaluable because of melanin interference. Considering the best cut-off resulting from the ROC curves analysis, values of CAF-1 p60 and CAF-1 p150 were classified as "HIGH" and "LOW," including negative cases in the "LOW" category.

Survival curves analysis showed a statistically significant difference between CAF-1p60^{HIGH} and CAF-1 p60^{LOW} for overall survival (log-rank test, $p < 0.0001$) and disease-free survival (p = 0.002).

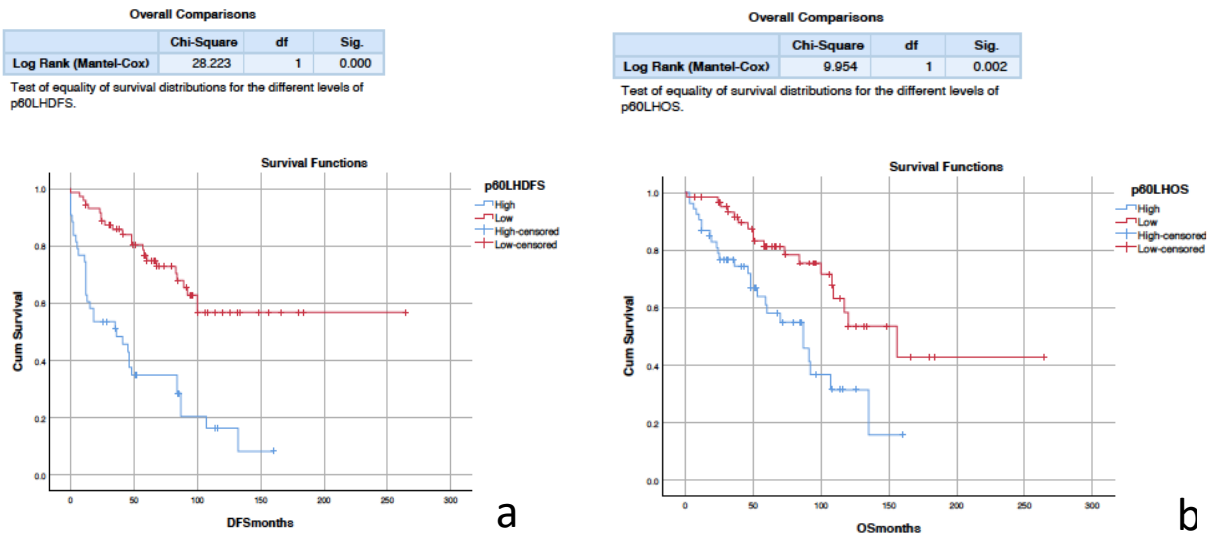

Figure 16: Kaplan Meier curves for disease free survival (a) and overall survival (b) related to CAF-1 p60 expression.

Similar results were observed for CAF-1p150 both for disease-free survival (DFS) and overall survival (OS) (p = 0.004 and p < 0.0001, respectively).

Overall Comparisons

	Chi-Square	df	Sig.
Log Rank (Mantel-Cox)	24.176	1	0.000

Test of equality of survival distributions for the different levels of p150LH.

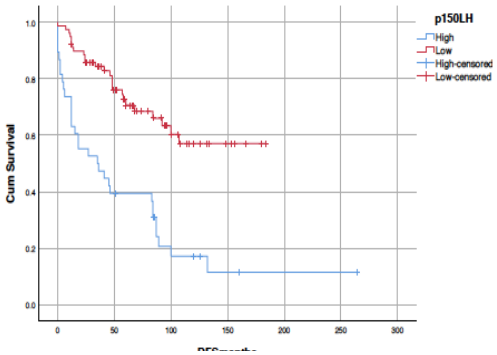

Figure 17:Kaplan Meier curves for disease free survival and CAF-1 p150 expression.

For both markers, the survival curves revealed that low or absent expression of these markers correlates with more prolonged disease-free survival and overall survival.

Overall Comparisons

	Chi-Square	df	Sig.
Log Rank (Mantel-Cox)	8.423	1	0.004

Test of equality of survival distributions for the different levels of p150LHOS.

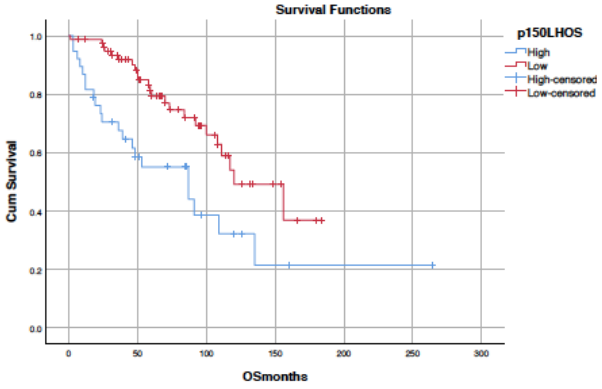

Figure 18: Kaplan Meier for overall survival and CAF-1 p150 expression.

Moreover, we created four clusters, considering both CAF-1p60 and CAF-1 p150 immunohistochemical expression. The four clusters were defined as p150 ^{HIGH}/p60 ^{HIGH}; p150^{LOW}/p60^{HIGH}; p150 ^{HIGH} /p60 ^{LOW} and p150^{LOW}/p60^{LOW} (table 2). We observed that p150 ^{HIGH}/p60 ^{HIGH} score correlates with a poor prognosis in terms of overall survival and disease-free survival in the whole tested population, while no significant differences were found in terms of demographics and histology. Kaplan-Meier curves were drawn using this grouping, with significant survival differences across the four categories (figure 14).

	HIGH/HIGH	*LOW/HIGH*	*HIGH/LOW*	*LOW/LOW*	*P VALUE*
SEX (M)	19 (46%)	5 (31%)	7 (50%)	27 (50%)	0,49
AGE (YEARS)	64±12	71±11	57±12	62±15	0,13
LBD (CM)	1,45±0,42	1,71±0,94	1,23±0,50	1,29±0,51	< 0,05
THICKNESS (CM)	0,93±0,39	0,95±0,36	0,83±0,40	0,75±0,45	0,38
TNM (T1/2/3/4)	3 / 9 / 18 / 10	1 / 4 / 7 / 3	2 / 4 / 6 / 2	15 / 15 / 13 / 11	0,61
CELLULARITY (EPITHELIOID / SPINDLE /MIXED)	11 / 4 / 26	6 / 1 / 9	3 / 4 / 8	15 / 10 / 31	0,60
METASTASIS/RECURRENCE	30 (73%)	4 (25%)	6 (40%)	16 (28%)	< 0,002
DISEASE-FREE SURVIVAL (MONTHS)	44±47	58±35	82±64	72±47	< 0,05
OVERALL SURVIVAL (MONTHS)	50±44	62±31	85±62	76±45	0,07

Table 2: Clinicopathologic features and survival of UM cases clustered according to the combined expression of CAF-1 p60 and CAF-1 p150.

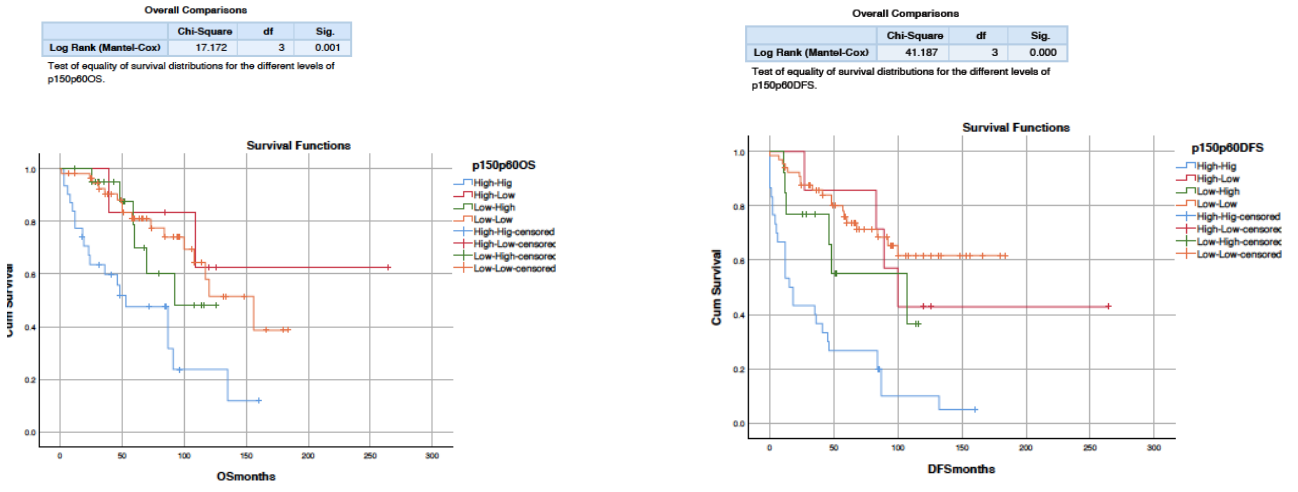

a b

Figure 19: Kaplan Meier curves for overall survival (a) and disease-free survival in categories based on the combined expression of CAF-1 p150 and CAF-1 p60.

Immunohistochemical evaluation of BAP1 resulted in less useful in prognostic stratification of patients.

Overall Comparisons

	Chi-Square	df	Sig.
Log Rank (Mantel-Cox)	,024	1	,878

Test of equality of survival distributions for the different levels of BAP1.

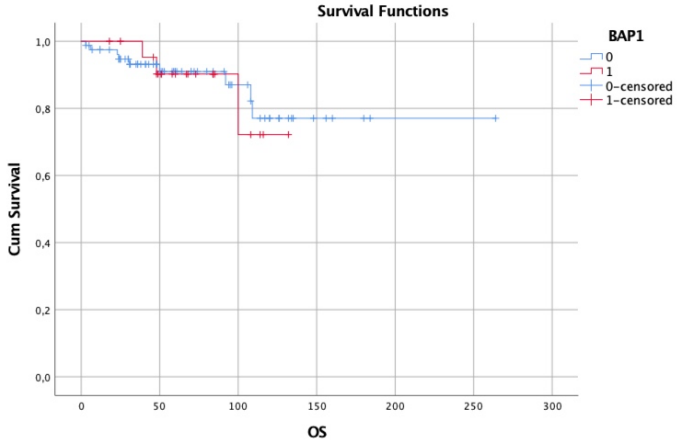

Figure 20: Kaplan Meier curves for overall survival depending on BAP-1 expression.

Discussion and Conclusions

UM is rare neoplasia characterized by unpredictable behavior. More than 50% of UM patients develop metastasis, and less than 4% present metastasis at the time of primary disease[16]. 20–30% of the patients develop metastatic disease within 5 years from diagnosis and almost 45% at 15 years[48]. Although it shares morphological features with its cutaneous counterpart, UM is entirely different neoplasia for genetic landscape, clinical behavior, and therapy responsiveness. UM has an extremely low mutational burden, and characteristic mutations of cutaneous melanoma such as BRAF and N-Ras, K-Ras, H-Ras, are rare. Therefore, most therapeutic strategies used in cutaneous melanoma resulted ineffective in metastatic UM with a very poor prognosis, after the diagnosis of metastatic disease and with only marginal improvements in survival in decades. Different prognostic strategies were elaborated based on pathological parameters and genetic alterations (GEP and TGCA classifications) in the last years. Although molecular predictive tests in UM have achieved a high level of precision, they still have little impact on treatment decisions. Moreover, prognostic molecular systems are studied ad validated on intraocular fine-needle aspiration biopsy (FNAB). Intraocular biopsy in ocular malignancies is still a matter of debate because of the risk of tumor dissemination and the risks related to the procedure's invasiveness. Insufficient sampling and potentially sight-threatening ocular complications, particularly in the case of small posterior tumors, are possibilities that should be considered before choosing this surgical approach[49].

Even if correctly performed in highly specialized centers, the most critical limitation of FNAB in UM is tumor heterogeneity. Tumor heterogeneity is a significant cause of misclassification related to the sampling procedure[34]. Moreover, the emotional impact of prognostication on patients should not be underestimated, given that treatment cannot change life expectancy[50].

Despite the mutational landscape of UM is well defined, the role of epigenetics in the UM is not equally characterized. Epigenetic alterations probably have an early role in carcinogenesis; therefore, they are considered a hallmark of cancer. Epigenetic mechanisms involved in cancer development are micro-RNA expression level variations, hypermethylation of tumor suppressor genes, hypomethylation of oncogenes, and histone modification patterns.

For these reasons, we focused in this research work on the Chromatin Assembly Factor 1 (CAF-1) complex, the most relevant factor involved in the inheritance of epigenetic information. Previous

researches assessed the immunohistochemical expression of CAF-1 subunits, demonstrating its potential role as prognostic markers in different solid tumors.

CAF-1 complex comprises three subunits, p48, responsible for the histone's acetylation and deacetylation, p60 involved in cell replication, and p150 mainly implicated in the DNA repair process.

We tested the immunohistochemical expression of CAF-1 p60 and CAF-1 p150 subunits in 133 cases of UM obtained from enucleations conducted between 1990 and 2018. For each case, we selected two or more areas considering the tumor heterogeneity[51]. We evaluated the immunohistochemical expression of CAF-1 subunits through a new, objective score system. We demonstrated the association with high expression of CAF-1 p60 and CAF-1 p150 with tumor recurrence, metastasis, and Shorter Overall Survival and Disease-Free Survival for both markers. Moreover, we tested the predictive efficacy of the combination of both markers.

We created four new clusters, considering both CAF-1p150 and CAF-1 p60 immunohistochemical expression. The four clusters were defined as $p150^{HIGH}/p60^{HIGH}$; $p150^{LOW}/p60^{HIGH}$; $p150^{HIGH}/p60^{LOW}$ and $p150^{LOW}/p60^{LOW}$. We observed that $p150^{HIGH}/p60^{HIGH}$ strongly correlates with a poor prognosis in terms of overall survival and disease-free survival. The immunohistochemical evaluation of CAF-1p150 and CAF-1p60 revealed as a reliable prognostic marker even if compared with BAP1[52], currently considered an important indicator of metastatic potential in this setting.

In conclusion, CAF-1 is a heterotrimeric complex with a well-established role in preserving heterochromatin and as a guardian of the cell identity. Unfortunately, its role in regulating gene expression and gene silencing is almost unexplored.

The immunohistochemical overexpression of CAF-1 p150 and CAF-1 p60 subunits in a large proportion of UM opens up the possibility of exploring the epigenetic role of this complex in the pathogenesis and acquisition of aggressive behavior and metastatic potential in this neoplasia. Moreover, the recent shreds of evidence of the CAF-1 complex involvement in the mechanism of target therapy resistance through epigenetics changes[53] provide new therapeutic insights.

Bibliography

1. Rodrigues, M. *et al.* So close, yet so far: Discrepancies between uveal and other melanomas. a position paper from UM cure 2020. *Cancers (Basel).* **11**, (2019).
2. Kivelä, T. T. The first description of the complete natural history of uveal melanoma by two Scottish surgeons, Allan Burns and James Wardrop. *Acta Ophthalmol.* **96**, 203–214 (2018).
3. Bakhoum, M. F. & Esmaeli, B. Molecular characteristics of uveal melanoma: Insights from the cancer genome atlas (TCGA) project. *Cancers* **11**, (2019).
4. Bakhoum, M. F. & Esmaeli, B. Molecular characteristics of uveal melanoma: Insights from the cancer genome atlas (TCGA) project. *Cancers* **11**, (2019).
5. Krantz, B. A., Dave, N., Komatsubara, K. M., Marr, B. P. & Carvajal, R. D. Uveal melanoma: Epidemiology, etiology, and treatment of primary disease. *Clinical Ophthalmology* (2017). doi:10.2147/OPTH.S89591
6. Grossniklaus HE, Eberhart CG, Kivelä TT. *WHO Classification of Tumours of the Eye*. e. Fourth Edition. International Agency for Research on Cancer. (2018)
7. Shields, C. L. *et al.* Uveal melanoma in children and teenagers. *Saudi J. Ophthalmol.* **27**, 197–201 (2013).
8. KATOPODIS, P., KHALIFA, M. S. & ANIKIN, V. Molecular characteristics of uveal melanoma and intraocular tumors (Review). *Oncol. Lett.* **21**, (2021).
9. Fallico, M. *et al.* Current molecular and clinical insights into uveal melanoma (Review). *Int. J. Oncol.* **58**, (2021).
10. Ferguson, R. *et al.* Genetic markers of pigmentation are novel risk loci for uveal melanoma. *Sci. Rep.* **6**, (2016).
11. Chalada, M., Ramlogan-Steel, C. A., Dhungel, B. P., Layton, C. J. & Steel, J. C. The impact of ultraviolet radiation on the aetiology and development of uveal melanoma. *Cancers* **13**, (2021).
12. Johansson, P. A. *et al.* Whole genome landscapes of uveal melanoma show an ultraviolet radiation signature in iris tumours. *Nat. Commun.* **11**, (2020).
13. Amaro, A. *et al.* The biology of uveal melanoma. *Cancer Metastasis Rev.* (2017). doi:10.1007/s10555-017-9663-3
14. Louie, B. H. & Kurzrock, R. BAP1: Not just a BRCA1-associated protein. *Cancer Treatment Reviews* **90**, (2020).
15. van Poppelen, N. M. *et al.* Genetics of ocular melanoma: Insights into genetics, inheritance

and testing. *International Journal of Molecular Sciences* **22**, 1–19 (2021).

16. Violanti, S. S. *et al.* New insights into molecular oncogenesis and therapy of uveal melanoma. *Cancers (Basel).* **11**, 1–25 (2019).
17. Laíns, I. *et al.* Second Primary Neoplasms in Patients With Uveal Melanoma: A SEER Database Analysis. *Am. J. Ophthalmol.* **165**, 54–64 (2016).
18. Yavuzyigitoglu, S. *et al.* Uveal Melanomas with SF3B1 Mutations: A Distinct Subclass Associated with Late-Onset Metastases. *Ophthalmology* **123**, 1118–1128 (2016).
19. Ortega, M. A. *et al.* Update on uveal melanoma: Translational research from biology to clinical practice (Review). *International Journal of Oncology* **57**, 1262–1279 (2020).
20. Mensink, H. W. *et al.* Chromosomal aberrations in iris melanomas. *Br. J. Ophthalmol.* **95**, 424–428 (2011).
21. Roberts, F. *Lee' s Ophthalmic Histopathology* 3rd ed. London: Springer 2014.
22. Uveal, M. : *NCCN.org NCCN Clinical Practice Guidelines in Oncology (NCCN Guidelines ®)*. (2021).
23. Jager, M. J. *et al.* Uveal melanoma. *Nat. Rev. Dis. Prim.* **6**, (2020).
24. Bochner, B.H., Hansel, D.E., Efstathiou, J.A., Konety, B., Lee, C.T., Mckiernan, J.M., Plimack, E.R., Reuter, V.E., Sridhar, S., Vikram, R., Stadler, W. M. *AJCC Cancer Staging Manual, 8th edition*. *American Joint Commitee on Cancer* (2017). doi:10.1007/978-3-319-40618-3
25. Shields, C. L. *et al.* Prognostication of uveal melanoma is simple and highly predictive using the Cancer Genome Atlas (TCGA) classification: A review. *Indian Journal of Ophthalmology* **67**, 1959–1963 (2019).
26. Mazloumi, M. *et al.* Accuracy of the Cancer Genome Atlas Classification vs American Joint Committee on Cancer Classification for Prediction of Metastasis in Patients with Uveal Melanoma. *JAMA Ophthalmol.* **138**, 260–267 (2020).
27. Shields, C. L. *et al.* American Joint Committee on Cancer classification of posterior uveal melanoma (tumor size category) predicts prognosis in 7731 patients. *Ophthalmology* **120**, 2066–2071 (2013).
28. Onken, M. D., Li, J. & Cooper, J. A. Uveal melanoma cells utilize a novel route for transendothelial migration. *PLoS One* **9**, (2014).
29. Patrone, S. *et al.* Prognostic value of chromosomal imbalances, gene mutations, and BAP1 expression in uveal melanoma. *Genes Chromosom. Cancer* **57**, 387–400 (2018).
30. Robertson, A. G. *et al.* Integrative Analysis Identifies Four Molecular and Clinical Subsets in

Uveal Melanoma. *Cancer Cell* **32**, 204-220.e15 (2017).

31. Jager, M. J., Brouwer, N. J. & Esmaeli, B. The Cancer Genome Atlas Project: An Integrated Molecular View of Uveal Melanoma. *Ophthalmology* **125**, 1139–1142 (2018).
32. Harbour, J. W. A prognostic test to predict the risk of metastasis in uveal melanoma based on a 15-gene expression profile. *Methods Mol. Biol.* (2014). doi:10.1007/978-1-62703-727-3_22
33. Field, M. G. *et al.* PRAME as an independent biomarker for metastasis in uveal melanoma. *Clin. Cancer Res.* (2016). doi:10.1158/1078-0432.CCR-15-2071
34. Fonseca, C. *et al.* Intratumoral Heterogeneity in Uveal Melanoma. *Ocul. Oncol. Pathol.* **7**, 17–25 (2021).
35. Yang, J., Manson, D. K., Marr, B. P. & Carvajal, R. D. Treatment of uveal melanoma: where are we now? *Ther. Adv. Med. Oncol.* (2018). doi:10.1177/1758834018757175
36. Smith, S. & Stillman, B. Purification and characterization of CAF-I, a human cell factor required for chromatin assembly during DNA replication in vitro. *Cell* (1989). doi:10.1016/0092-8674(89)90398-X
37. Volk, A. & Crispino, J. D. The role of the chromatin assembly complex (CAF-1) and its p60 subunit (CHAF1b) in homeostasis and disease. *Biochim. Biophys. Acta - Gene Regul. Mech.* **1849**, 979–986 (2015).
38. Nabatiyan, A. & Krude, T. Silencing of chromatin assembly factor 1 in human cells leads to cell death and loss of chromatin assembly during DNA synthesis. *Mol. Cell. Biol.* (2004). doi:10.1128/MCB.24.7.2853
39. Moggs, J. G. *et al.* A CAF-1-PCNA-Mediated Chromatin Assembly Pathway Triggered by Sensing DNA Damage. *Mol. Cell. Biol.* (2000). doi:10.1128/MCB.20.4.1206-1218.2000
40. Hoek, M., Myers, M. P. & Stillman, B. An analysis of CAF-1-interacting proteins reveals dynamic and direct interactions with the KU complex and 14-3-3 proteins. *J. Biol. Chem.* **286**, 10876–10887 (2011).
41. Staibano, S. *et al.* Chromatin assembly factor-1 (CAF-1)-mediated regulation of cell proliferation and DNA repair: A link with the biological behaviour of squamous cell carcinoma of the tongue? *Histopathology* **50**, 911–919 (2007).
42. Staibano, S. *et al.* The proliferation marker Chromatin Assembly Factor-1 is of clinical value in predicting the biological behaviour of salivary gland tumours. *Oncol. Rep.* (2011). doi:10.3892/or-00001036

43. Mascolo, M. *et al.* Overexpression of Chromatin Assembly Factor-1/p60 helps to predict the prognosis of melanoma patients. *BMC Cancer* **10**, 63 (2010).
44. Yang, S., Long, Q., Chen, M., Liu, X. & Zhou, H. CAF-1/p150 promotes cell proliferation, migration, invasion and predicts a poor prognosis in patients with cervical cancer. *Oncol. Lett.* **20**, 2338–2346 (2020).
45. Kucherlapati, M. Examining transcriptional changes to DNA replication and repair factors over uveal melanoma subtypes. *BMC Cancer* **18**, 818 (2018).
46. Remotti, H. Tissue microarrays: Construction and use. *Methods Mol. Biol.* **980**, 13–28 (2013).
47. Sun, M. *et al.* Prediction of BAP1 expression in uveal melanoma using densely-connected deep classification networks. *Cancers (Basel).* **11**, (2019).
48. Croce, M., Ferrini, S., Pfeffer, U. & Gangemi, R. Targeted therapy of uveal melanoma: Recent failures and new perspectives. *Cancers* **11**, (2019).
49. Frizziero, L. *et al.* Uveal melanoma biopsy: A review. *Cancers* **11**, (2019).
50. Brown, S. L. *et al.* Is accurate routine cancer prognostication psychologically harmful? 5-year outcomes of life expectancy prognostication in uveal melanoma survivors. *J. Cancer Surviv.* 1–13 (2021). doi:10.1007/s11764-021-01036-4
51. Fonseca, C. *et al.* Intratumoral Heterogeneity in Uveal Melanoma. *Ocul. Oncol. Pathol.* **7**, 17–25 (2021).
52. Szalai, E., Wells, J. R., Ward, L. & Grossniklaus, H. E. Uveal Melanoma Nuclear BRCA1-Associated Protein-1 Immunoreactivity Is an Indicator of Metastasis. *Ophthalmology* **125**, 203–209 (2018).
53. Wang, Z. *et al.* Chromatin assembly factor 1 suppresses epigenetic reprogramming toward adaptive drug resistance. *J. Natl. Cancer Cent.* **1**, 15–22 (2021).